Hierarchical Nanoparticles

International Edition: DOI: 10.1002/anie.201511768
German Edition: DOI: 10.1002/ange.201511768

Solution-Based Fabrication of Narrow-Disperse ABC Three-Segment and Θ-Shaped Nanoparticles

*Zhen Zhang[+], Changming Zhou[+], Haiyan Dong, and Daoyong Chen**

Abstract: *Nanoparticles sized tens of nm with not only a highly complex but also a highly regular nanostructure, although ubiquitous in nature, are very difficult to prepare artificially. Herein, we report efficient solution-based preparation of narrow-disperse ABC three-segment hierarchical nanoparticles (HNPs) with a size of tens of nm through a three-level hierarchical self-assembly of A-b-B-b-C triblock copolymers in solution. An ABC HNP is composed of three nanoparticles, A, B, and C that are linearly connected; in the ABC HNP, the B nanoparticle is sandwiched between the A and C nanoparticles. The method for the preparation is highly efficient, because all of the A-b-B-b-C chains in the solution are converted into the ABC HNPs. Furthermore, the ABC HNPs self-assembled into Θ-shaped HNPs tens nm in size. Both the ABC and Θ-shaped HNPs, are highly complex but highly regular, and are novel HNPs, and they should be very promising for addressing various theoretical and practical problems.*

Current and prospective developments in nanoscience and nanotechnology require nanostructures with not only high complexity but also high regularity whose fabrications in turn pose great challenges.[1] Of the nanostructures, hierarchically nanostructured polymeric nanoparticles (HNPs) have attracted much attention in the fields of biological and medical sciences, physical chemistry, polymer science, and chemical self-assembly.[2] For applications, HNPs are believed as more versatile platforms than simply structured nanoparticles such as micelles and vesicles, because HNPs can transport different payloads simultaneously and thus possibly deliver various agents in a designed stoichiometric ratio.[2e] Moreover, HNPs have significant similarities to proteins because both of them contain multi-nanocompartments, and are formed by the multi-levelled hierarchical self-assembly driven by multi-orthogonal interactions. Studies of HNPs are helpful for deeply understanding formation mechanism of biological nanostructures and mimicking their structures and functions. Over past few years, much research has been carried out on preparing HNPs.[2d,e,3] Through self-assembly of multicomponent polymers, many kinds of HNPs, such as hamburger-like NPs,[3c] spherical and linear multicompartment micelles,[4] sub-structured vesicles,[5] cylindrical block co-micelles[3a,e,6] and bicontinuous micelles[7] have been reported.[8] Among such HNPs, those with narrow-dispersity, high complexity but high regularity are especially desirable because they are more ideal mimics of bio-nanostructures, and the narrow-dispersity allows their further self-assembly into even more complex but regular nanostructures.[2d,e] However, these specific HNPs are rarely reported and their synthesis, particularly for the sub-100 nm ones, remains a challenge.

Herein, we report highly efficient solution-based preparation of narrow-disperse ABC three-segment HNPs, a novel type of HNPs through following a three-level hierarchical self-assembly processes: 1) Self-assembly of A-*b*-B-*b*-C triblock copolymers to form mixed shell micelles (MSMs) with a relatively large and dynamic core formed by the B block chains and an A/C mixed shell (Figure 1 a,b); 2) Intramicellarly crosslinking the A (or C) chains to convert one MSM into one Janus NP (Figure 1 c); and 3) Further structural evolution from the Janus NPs to ABC three-segment HNPs (Figure 1 d). This method for preparing ABC HNPs is highly efficient because almost all of the A-*b*-B-*b*-C chains in the solution are converted to the ABC HNPs. Furthermore, ABC HNPs can self-assemble into the HNPs with a Θ-like morphology (Figure 1 e,f). Both ABC and Θ-like HNPs are novel HNPs, and are highly complexly but regularly structured; nanostructures (with a size below 100 nm) with not

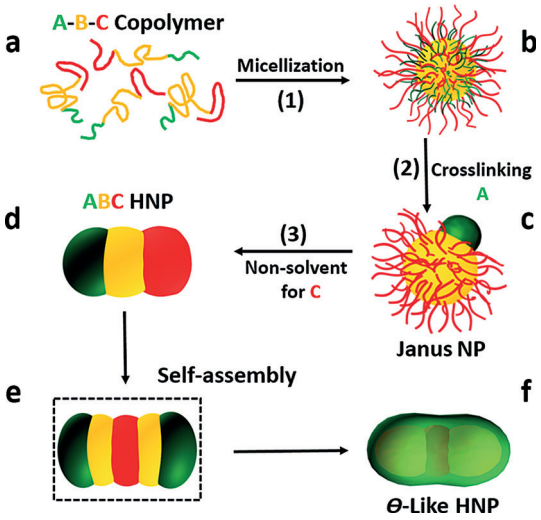

Figure 1. Schematic illustration of the hierarchical self-assembly for preparing the ABC three-segment HNPs (a–d) and their further self-assembly into Θ-shaped HNPs (e–f). For steps 1–3 see text for details

[*] Z. Zhang,[+] C. Zhou,[+] H. Dong, D. Chen
The State Key Laboratory of Molecular Engineering of Polymers and Department of Macromolecular Science, Fudan University
220 Handan Road, Shanghai 200433 (P.R. China)
E-mail: chendy@fudan.edu.cn

[+] These authors contributed equally to this work.

Supporting information for this article can be found under: http://dx.doi.org/10.1002/anie.201511768.

only a high complexity but also a high regularity, although they are common in nature, are seldom obtained artificially.

A commercially available triblock copolymer polystyrene-*block*-polybutadiene (1,4-addition) -*block*-poly(2-vinylpyridine) (PS_{440}-*b*-PB_{1019}-*b*-$P2VP_{114}$, (SBV), subscripts represent the average degrees of polymerization; $M_w/M_n = 1.06$) was used to prepare the MSMs (Figure 1 a,b). *N*,*N*-dimethylformamide (DMF) was chosen as the selective solvent for the P2VP and PS block chains (See S2 in the Supporting information).[9] In DMF, the Hydrodynamic radius $< R_h >$ of the SBV nanoaggregates measured by dynamic light scattering (DLS) was 47 nm (Figure 2 a, red line), which is much

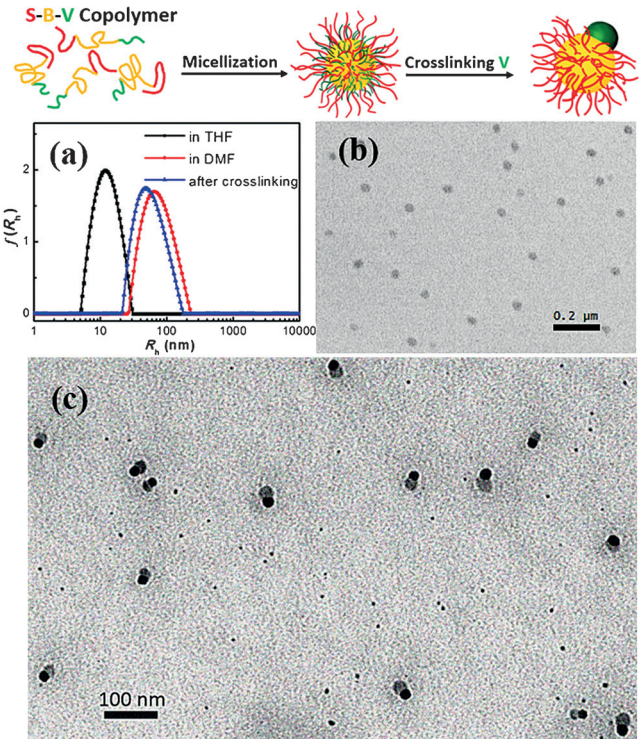

Figure 2. Top: schematic representation of micellization and crosslinking. a) Hydrodynamic radius distributions of SBV in THF (black), the SBV MSMs formed in DMF (red), and the crosslinked SBV MSMs in DMF (blue); b) TEM image of SBV MSMs formed in DMF (without staining); c) TEM image of the crosslinked MSMs in DMF (stained by $AgNO_3$).

larger than that of the SBV single chain in THF (11 nm; Figure 2 a and S2 in SI). Clearer, SBV underwent self-assembly in DMF to form multi-chain aggregates. The TEM observations showed that the SBV aggregates were spherical micelles with a diameter of approximately 42 nm (Figure 2 b); the size determined by TEM was much less than that by DLS, which can be explained by the contraction of the micelles in the dried state. According to the GPC-MALLS measurements using DMF as the eluent, the micelles had an M_w of $2.2 \times 10^7\ g\,mol^{-1}$. Because the M_w value of the SBV single chain was $1.11 \times 10^5\ g\,mol^{-1}$, it was calculated that each micelle was composed of approximately 200 polymer chains, which was a reasonable aggregation number of polymer chains in a block copolymer micelle.[9c,10]

Because DMF is a good solvent for PS and P2VP but a non-solvent for PB,[9,11] the SBV micelles formed in DMF are MSMs with the PB block chains as the core, and the PS and P2VP block chains are the mixed shell. Compared to the P2VP block chains, the PS block chains are long, and the PB core is large, because the PS/P2VP length ratio and PB/P2VP weight ratio is 3.9/1 and 4.6/1, respectively. Additionally, the core is dynamic because PB is in a rubber state at room temperature.

The P2VP block chains in the mixed shell of the SBV MSMs were crosslinked in DMF by using 1,4-dibromobutane (DBB) as the crosslinker.[9a,b] The $< R_h >$ of the crosslinked MSMs measured by DLS was 44 nm (Figure 2 a, blue line), which is slightly smaller than the $< R_h >$ of the not crosslinked MSMs (47 nm). The M_w of the crosslinked MSMs measured by GPC-MALLS using DMF as the eluent was $2.7 \times 10^7\ g\,mol^{-1}$, which is slightly larger than the M_w of the not crosslinked MSMs ($2.2 \times 10^7\ g\,mol^{-1}$). By analyzing the changes in $< R_h >$ and M_w of the MSMs before and after the crosslinking, it can be concluded that the crosslinking of the P2VP block chains occurred intramicellarly; the slight increase in M_w was attributed to the incorporation of the crosslinker into the MSMs during crosslinking (S3 in SI). It is conceivable that if there had been considerable intermicellar crosslinking in the system, then both the $< R_h >$ and M_w of the aggregates in the system would have been significantly increased. The intramicellar crosslinking is understandable by considering the fact that, in the mixed shell of the MSMs, the PS/P2VP length ratio is 3.9/1; the protection of the long PS block chains effectively prevented intermicellar crosslinking of the P2VP chains, so that the crosslinking of P2VP occurred intramicellarly. The intramicellar crosslinking is also consistent with the results reported by Liu and Armes[12] and Wooley et al.[13] (S4 in SI).

The intramicellarly crosslinked MSMs (CMSMs) were observed by TEM. In the TEM images of the CMSMs stained by $AgNO_3$ (S5 in SI),[14] all of the CMSMs were narrow-disperse Janus NPs with a length about 42 nm (Figure 2 c, S6 and S7 in SI); the relatively large difference in the sizes determined by TEM and DLS can be attributed to the contraction of the Janus particles in the dried state. The spherical domain with high contrast was formed by crosslinked P2VP; the reaction between $AgNO_3$ and the $N^+B_r^-$ (N^+ represents a quaternized pyridine unit) units led to formation of AgBr within the crosslinked network and thus enhanced the contrast of the domain. The domain with low contrast was composed of PS block chains; the Ag^+–π interaction between the Ag^+ of $AgNO_3$ and the benzene rings of the PS resulted in contrast enhancement in the PS-containing domains.[15] The PB core was encapsulated because the PB block chains were insoluble in the solvent DMF. The abovementioned facts that the molecular weight and size of the Janus NPs (the CMSMs) were similar to those of the precursor MSMs reveal that the conversion from the MSMs into the Janus NPs (CMSMs) was a one-to-one conversion, which was realized by intramicellarly crosslinking all of the P2VP chains in an MSM together into one domain (S6 in SI). We repeated the one-to-one conversion from the SBV MSMs into the SBV Janus NPs several times, and the same results

were obtained (S8 in SI). TEM observations demonstrate that almost all of the block copolymer in the solution was converted into the Janus NPs. Therefore, the present study exhibits a novel, reliable and highly efficient solution-based method that can be used not only for fabricating ABC three-segment HNPs (detailed below), but also for preparing Janus NPs sized tens nm (S9 in SI). It should be mentioned that the methods that can be used for the solution-based preparation of Janus NPs with a size of tens of nm are still very limited.[16]

The mechanism for conversion from the MSMs into the Janus NPs is clear. In the present study, the PB core is large and dynamic, whereas the crosslinkable P2VP block chains in the shell are relatively short. Therefore, the crosslinked P2VP block chains cannot form an integrated shell to cover the entire surface of the core. At the early stage of the intramicellar crosslinking, multiple small crosslinked P2VP domains form in each MSM (S10a in SI). It is significant that, at the late stage, facilitated by the large and dynamic core (S10b in SI), the crosslinking forces all of the P2VP block chains in the mixed shell to aggregate together into one domain at one side of the core, and at the same time, the not-crosslinkable PS block chains in the shell are largely excluded from the crosslinked network. Thus, conversion of one MSM into one Janus NP was realized.

The method for preparing SBV Janus NPs is different from the method reported in literature (S9a in SI); strong interaction (crosslinking) was applied to induce complete phase separation between the P2VP and the PS block chains in the mixed shell (S9b in SI). Besides, the SBV Janus NPs have the following unique structure: in a SBV Janus NP prepared in the present study, the NP formed by approximately 200 crosslinked $P2VP_{114}$ block chains, as one side of the Janus NP, is grafted only on one side by the same number of the PB_{1019}-*b*-PS_{440} diblock chains (Figure 1c; as mentioned above, an SBV Janus NP (a CMSM) was formed by around 200 SBV triblock copolymer chains). The unique structure not only makes the Janus NPs different from the other Janus NPs formed by triblock copolymers (S9c in SI), but also allows for their further structural evolution into the three-segment HNPs. After addition of methanol into suspension of the SBV Janus NPs in DMF (0.5 mg mL^{-1}) to the methanol/DMF volume ratio of 0.30 (S11 in SI), according to TEM and AFM observations, the SBV Janus NPs were transformed to the narrow-disperse SBV three-segment HNPs with a length about 64 nm (S12 in SI). The length observed by TEM was much less than the size measured by DLS ($<R_h>=40$ nm, Figure 3a), which can also be accounted for by the contraction of the particles in the dried state. In the TEM images (Figure 3c and Figure S5), the relatively small high contrast domain is the crosslinked P2VP domain (the V segment), the relatively large domain with a high contrast is the PS domain (the S segment), and the low-contrast domain located between the S and V segments is the PB domain (B segment). AFM observations also demonstrated that the NPs were SBV three segment HNPs (Figure 3b and S13a in SI). In the AFM image of SBV HNPs, it is exhibited that the central PB segment is thinner than the P2VP and PS segments (S13a in SI). This phenomenon should result from compression of the PB segment in the rubber state by the tapping-mode AFM

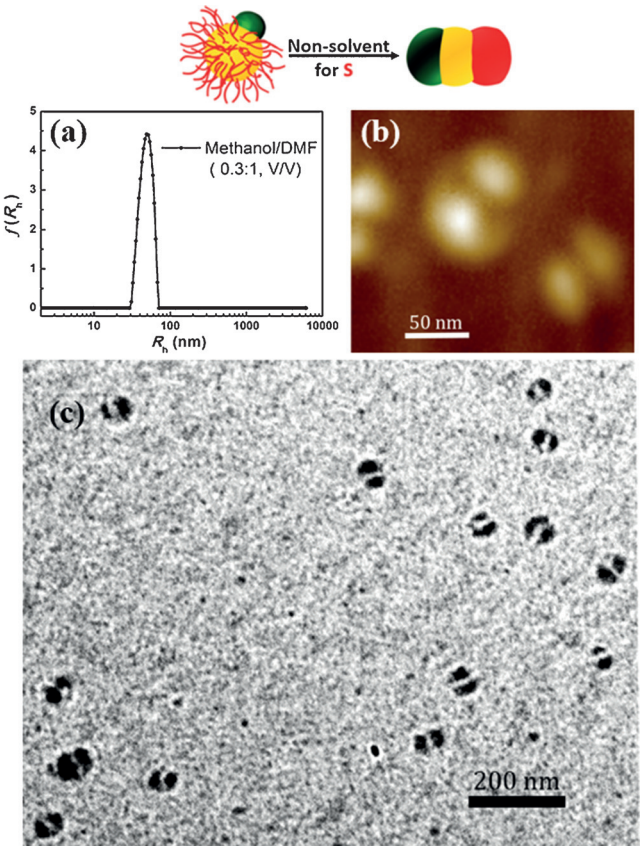

Figure 3. a) Hydrodynamic radius distribution of the SBV three-segment HNPs formed in methanol/DMF (0.30/1.0, *v*/*v*). b) AFM and c) TEM images (without staining) of the SBV three-segment HNPs formed in methanol/DMF (0.30/1, *v*/*v*) mixed solvent.

measurements (S13a,b in SI). Both the TEM observations (Figure 3c, Figure S5 and S12) and the DLS results (Figure 3a) demonstrate that the SBV three-segment HNPs are narrow-disperse. Clearly, an SBV HNP is a bundle of around 200 orderly arranged PS_{440}-*b*-PB_{1019}-*b*-$P2VP_{114}$ chains: the same number (ca. 200) of PS_{440}, PB_{1019}, and crosslinked $P2VP_{114}$ block chains in the bundle form the S, B, or V segments, respectively; in the SBV three-segment HNPs, the B segment is sandwiched between the S and the V segments. Therefore, the ABC three-segment HNPs are a novel type of HNPs. TEM observations confirmed that almost all of the SBV triblock copolymer used was converted into the SBV HNPs; the method is highly efficient. The conversion from random coils of the SBV triblock copolymer in THF into the SBV three-segment NPs was repeatedly conducted in several separate batches, and similar results were obtained (Figure S5).

Significantly, after further adding methanol to the suspension of SBV NPs to increase the methanol/DMF volume ratio to 0.36/1.0, the HNPs with a Θ-like morphology and a size below 100 nm were obtained (Figure 4c). The formation mechanism of the Θ-shaped HNPs is also clear: the SBV HNPs dimerized into VBSBV penta-segment HNPs at the methanol/DMF volume ratio of 0.34/1.0 (Figure 4a,b and S14a in SI), and then, after the methanol/DMF volume ratio was further increased to 0.36, VBSBV HNPs changed to the

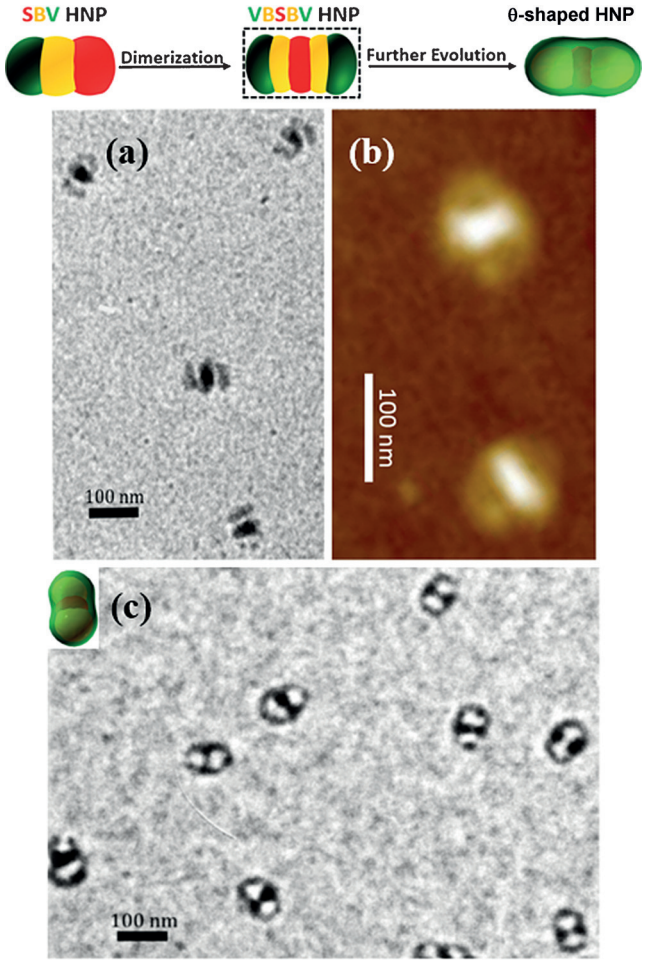

Figure 4. TEM (a) and AFM (b) images of the VBSBV HNPs formed at a methanol/DMF volume ratio of 0.34/1.0; c) TEM image of the Θ-like HNPs formed at a methanol/DMF volume ratio of 0.36/1.0; the inset at the top left corner of (c) shows the assignment of the domains in a Θ-shaped NP (the TEM images (a) and (c) were acquired without staining the samples).

Θ-shaped HNPs (S14b in SI). As indicated by the inset in Figure 4c, in a Θ-shaped HNP, two swollen V domains formed the shell (the green shell, Figure 4), the S domain (the red domain) is located at the central area, and the two B domains (the two yellow domains) are located at the two sides of the PS domain to form the two compartments in the Θ-shaped HNPs. In the TEM images (without staining) using the copper grids coated with ultrathin carbon film, the crosslinked P2VP and PS domains are visible, but the PB domains are invisible. The Θ-shaped HNPs can also be reproduced and with a relatively narrow size distribution (S15 in SI). We also crosslinked the PB domains of the Θ-shaped HNPs by the photo-crosslinking reaction (S16 in SI) to stabilize the Θ-shaped HNPs in the medium and enhance the contrast of the PB domains in the TEM images. As result, the inverse Θ-shaped HNPs were observed by TEM, confirming that the Θ-shaped HNPs were formed in the solution (S16 in SI).

In conclusion, we have developed hierarchical self-assembly processes for fabricating ABC three-segment HNPs, and HNPs with a Θ-shaped morphology. Both the ABC HNPs and the Θ-shaped HNPs are novel HNPs and are highly complexly but highly regularly nanostructured, which could considerably expand the morphologies of block-copolymer assemblies. Moreover, we also demonstrated that in this hierarchical self-assembly all of the processes can be well-controlled. The present study could inspire a more in-depth understanding of the formation mechanism of highly complex but regular hierarchical nanostructures and their manipulation, and be of interest in fields including bio and material sciences, *meso*-physics, nanotechnology, and polymer physics and chemistry.

Acknowledgements

We are grateful for the financial support from NSFC (21334001 and 21574025).

Keywords: copolymers · hierarchical nanoparticles · hierarchical self-assembly · nanoparticles

How to cite: *Angew. Chem. Int. Ed.* **2016**, *55*, 6182–6186
Angew. Chem. **2016**, *128*, 6290–6294

[1] a) R. F. Service, *Science* **2005**, *309*, 95; b) Y. Mai, A. Eisenberg, *Chem. Soc. Rev.* **2012**, *41*, 5969–5985; c) A. Walther, A. H. E. Müller, *Chem. Rev.* **2013**, *113*, 5194–5261; d) S. Mann, *Nat. Mater.* **2009**, *8*, 781–792; e) C. N. R. Rao, S. R. C. Vivekchand, K. Biswas, A. Govindaraj, *Dalton Trans.* **2007**, 3728–3749.

[2] a) Q. Chen, S. C. Bae, S. Granick, *Nature* **2011**, *469*, 381–384; b) Z. L. Zhang, S. C. Glotzer, *Nano Lett.* **2004**, *4*, 1407–1413; c) T. M. Hermans, M. A. C. Broeren, N. Gomopoulos, S. van der, M. H. P. van Genderen, N. A. J. M. Sommerdijk, G. Fytas, E. W. Meijer, *Nat. Nanotechnol.* **2009**, *4*, 721–726; d) A. H. Gröschel, A. Walther, T. I. Löbling, F. H. Schacher, H. Schmalz, A. H. E. Müller, *Nature* **2013**, *53*, 247–251; e) A. H. Gröschel, F. H. Schacher, H. Schmalz, O. V. Borisov, E. B. Zhulina, A. Walther, A. H. E. Müller, *Nat. Commun.* **2012**, *3*, 710; f) K. L. Young, M. L. Personick, M. Engel, P. F. Damasceno, S. N. Barnaby, R. Bleher, T. Li, S. C. Glotzer, B. Lee, C. A. Mirkin, *Angew. Chem. Int. Ed.* **2013**, *52*, 13980–13984; *Angew. Chem.* **2013**, *125*, 14230–14234.

[3] a) H. Qiu, Z. M. Hudson, M. A. Winnik, I. Manners, *Science* **2015**, *347*, 1329–1332; b) J. Zhu, S. Zhang, F. Zhang, K. L. Wooley, D. J. Pochan, *Adv. Funct. Mater.* **2013**, *23*, 1767–1773; c) J. Dupont, G. Liu, *Soft Matter* **2010**, *6*, 3654–3661; d) B. Fang, A. Walther, A. Wolf, Y. Xu, J. Yuan, A. H. E. Müller, *Angew. Chem. Int. Ed.* **2009**, *48*, 2877–2880; *Angew. Chem.* **2009**, *121*, 2921–2924; e) H. Qiu, G. Russo, P. A. Rupar, L. Chabanne, M. A. Winnik, I. Manners, *Angew. Chem. Int. Ed.* **2012**, *51*, 11882–11885; *Angew. Chem.* **2012**, *124*, 12052–12055.

[4] a) N. Saito, C. Liu, T. P. Lodge, M. A. Hillmyer, *ACS Nano* **2010**, *4*, 1907–1912; b) S. Kubowicz, J.-F. Baussard, J.-F. Lutz, A. F. Thünemann, H. von Berlepsch, A. Laschewsky, *Angew. Chem. Int. Ed.* **2005**, *44*, 5262–5265; *Angew. Chem.* **2005**, *117*, 5397–5400.

[5] Z. Li, M. A. Hillmyer, T. P. Lodge, *Langmuir* **2006**, *22*, 9409–9417.

[6] H. Cui, Z. Chen, S. Zhong, K. L. Wooley, D. J. Pochan, *Science* **2007**, *317*, 647–650.

[7] a) K. Hales, Z. Chen, K. L. Wooley, D. J. Pochan, *Nano Lett.* **2008**, *8*, 2023–2026; b) A. L. Parry, P. H. H. Bomans, S. J. Holder, N. A. J. M. Sommerdijk, S. C. G. Biagini, *Angew. Chem. Int. Ed.* **2008**, *47*, 8859–8862; *Angew. Chem.* **2008**, *120*, 8991–8994.

[8] a) T. Smart, H. Lomas, M. Massignani, M. V. Flores-Merino, L. R. Perez, G. Battaglia, *Nano Today* **2008**, *3*, 38 – 46; b) S. J. Holder, N. A. J. M. Sommerdijk, *Polym. Chem.* **2011**, *2*, 1018 – 1028.
[9] a) L. Cheng, G. Hou, J. Miao, D. Chen, M. Jiang, L. Zhu, *Macromolecules* **2008**, *41*, 8159 – 8166; b) T. Hui, D. Chen, M. Jiang, *Macromolecules* **2005**, *38*, 5834 – 5837; c) H. Iatrou, N. Hadjichristidis, G. Meier, H. Frielinghaus, M. Monkenbusch, *Macromolecules* **2002**, *35*, 5426 – 5437.
[10] S. Förster, M. Zisenis, E. Wenz, M. Antonietti, *J. Chem. Phys.* **1996**, *104*, 9956.
[11] L. Friebe, O. Nuyken, H. Windisch, W. Obrecht, *Macromol. Mater. Eng.* **2003**, *288*, 484 – 494.
[12] S. Liu, S. P. Armes, *J. Am. Chem. Soc.* **2001**, *123*, 9910 – 9911.
[13] K. B. Thurmond, T. Kowalewski, K. L. Wooley, *J. Am. Chem. Soc.* **1996**, *118*, 7239 – 7240.
[14] a) Y. Habata, A. Taniguchi, M. Ikeda, T. Hiraoka, N. Matsuyama, S. Otsuka, S. Kuwahara, *Inorg. Chem.* **2013**, *52*, 2542 – 2549; b) V. Sambhy, M. M. MacBride, B. R. Peterson, A. Sen, *J. Am. Chem. Soc.* **2006**, *128*, 9798 – 9808.
[15] a) Y. Lu, Y. Mei, M. Drechsler, M. Ballauff, *Angew. Chem. Int. Ed.* **2006**, *45*, 813 – 816; *Angew. Chem.* **2006**, *118*, 827 – 830; b) I. Ino, L. P. Wu, M. Munakata, T. Kuroda-Sowa, M. Maekawa, Y. Suenaga, R. Sakai, *Inorg. Chem.* **2000**, *39*, 5430 – 5436.
[16] A. H. Gröschel, A. Walther, T. I. Löbling, J. Schmelz, A. Hanisch, H. Schmalz, A. H. E. Müller, *J. Am. Chem. Soc.* **2012**, *134*, 13850 – 13860.

Received: December 19, 2015
Revised: March 1, 2016
Published online: April 13, 2016

